

doi:10.15199/48.2018.09.24

Measurement of the thickness of the oxygen-depleted layer in the $\text{Ag}/\text{YBa}_2\text{Cu}_3\text{O}_{7-x}/\text{Ag}$ structures of the electro-resistance memory

Abstract. The paper presents the results of experimental investigations of the phenomenon of electro-resistance memory in the $\text{Ag}/\text{YBa}_2\text{Cu}_3\text{O}_{7-x}/\text{Ag}$ thin-film structure at room and liquid nitrogen temperature. On the basis of the obtained voltage-current and amplitude characteristics, the threshold values of the resistive switching voltage were determined. Differences in the levels of these voltages at different switching directions and temperatures are explained using a mechanism based on oxygen ion electro-diffusion via oxygen vacancies. Using the mathematical model of this mechanism on the basis of the switching voltage values obtained, the thickness of layers depleted in oxygen ions were determined, which play a fundamental role in the switching process. The obtained thicknesses from 1.2 to 10.6 nm are consistent with the literature data for similar structures.

Streszczenie. W pracy przedstawiono wyniki badań doświadczalnych zjawiska pamięci elektrozystancyjnej w strukturze cienkowarstwowej $\text{Ag}/\text{YBa}_2\text{Cu}_3\text{O}_{7-x}/\text{Ag}$ w temperaturze pokojowej i ciekłego azotu. Na podstawie uzyskanych charakterystyk napięciowo-prądowych i amplitudowych wyznaczono wartości progowe napięcia przełączania rezystancji. Różnice poziomów tych napięć przy różnych kierunkach przełączania oraz temperaturach wyjaśniono za pomocą mechanizmu opartego na elektrodyfuzji jonów tlenu poprzez wakansy tlenowe. Wykorzystując model matematyczny tego mechanizmu na podstawie otrzymanych wartości napięcia przełączania wyznaczono grubości warstw zubożonych w jony tlenu, które odgrywają zasadniczą rolę w procesie przełączania. Otrzymane grubości od 1,2 do 10,6 nm są zgodne z danymi literaturowymi dla podobnych struktur. (Pomiar grubości warstwy zubożonej w tlen w strukturach $\text{Ag}/\text{YBa}_2\text{Cu}_3\text{O}_{7-x}/\text{Ag}$ pamięci elektrozystancyjnej).

Keywords: high-temperature superconductors, the phenomenon of electro-resistive memory, switching voltage, oxygen-ion electro-diffusion, depleted layer.

Słowa kluczowe: nadprzewodniki wysokotemperaturowe, zjawisko pamięci elektrozystancyjnej, napięcie przełączania, elektrodyfuzja jonów tlenu, warstwa zubożona.

Introduction

The constant development of computer technology requires better and better memories, both operational and mass. The requirements for devices of these two types are different. Operational memories must be quick, first of all, and they do not have to be the cheapest and can be volatile. In turn, mass storage must have huge capacities, low production and operating costs, and be non-volatile and have long life time. The requirements for the speed of writing and reading information are lower here than for the operational memory. Existing memories have already reached practically their physical limits. Therefore, in recent years, we can observe increased research activity in the search for new materials and phenomena that could be used to build memory elements. The analysis of development trends in this area, carried out in [1, 2], led to the isolation of ten new technologies that could soon replace the traditional ones.

In the field of mass storage, one of the most promising directions seems to be the use of the phenomenon of electro-resistive memory. This phenomenon occurs in many materials and at different temperatures (from 4 to 400K). Examples are oxide materials with a regular crystallographic structure, such as: TiO_2 [3], NiO , Al_2O_3 [4,5], or having a more complex perovskite structure: $\text{YBa}_2\text{Cu}_3\text{O}_{7-x}$ [6-9], $\text{Bi}_2\text{Sr}_2\text{CaCu}_2\text{O}_{8+\delta}$ [10], $\text{Pr}_{1-x}\text{Ca}_x\text{MnO}_3$ [11], $\text{La}_{1-x}\text{Sr}_x\text{CoO}_3$ [12], SrTiO_3 [13]. The latter also exhibit the properties of high-temperature superconductors (HTS). Superconducting materials have long tempt with low energy losses and high reaction rates.

The simplicity of the design of the electro-resistive memory element allows its far-reaching miniaturization (~10nm), which leads to a significant increase in capacity and low production costs. The phenomenon of electro-resistive memory is by nature non-volatile, so it does not require energy to store information. For recording and reading, currents of 10 μA are sufficient, which means low energy consumption and also promotes miniaturization. Another advantage of this type of memory is the possibility

of obtaining more than two of its states [14]. Multi-bit memories allow for additional capacity increase. Already today, materials are known in which switching times of resistive states are less than 50 ns, and therefore quite sufficient for mass memories. At present, the limits of the physical capabilities of electro-resistive memories are not completely known. Knowledge about switching mechanisms and preservation of memory states is also insufficient.

The aim of this work is to present the results of experimental research of resistance switching processes in a thin-film structure based on the high-temperature superconductor $\text{YBa}_2\text{Cu}_3\text{O}_{7-x}$ subjected to electric current. Particular interest was directed at determining the thickness of the oxygen-depleted layer, which plays an essential role in the switching mechanism.

Experiment

The study examined a sample in the form of HTS structure consisting of a thin film of the superconductor $\text{YBa}_2\text{Cu}_3\text{O}_{7-x}$ applied on a sapphire substrate (Al_2O_3) with dimensions of 10x6 mm [15]. The superconductor layer with a thickness of $h \approx 0.5 \mu\text{m}$ was obtained by magnetron sputtering. Crystallographic studies have shown the predominant orientation of the crystallite axis c perpendicular to the plane of the film. Next, the HTS film was formed by a microbridge-shaped photolithography with a width of $w = 200 \mu\text{m}$ and a length of $l = 2 \text{mm}$, and layers of silver contacts were sputtered and formed ($\text{Ag}/\text{YBa}_2\text{Cu}_3\text{O}_{7-x}/\text{Ag}$ structure). The parameters of the HTS microbridge measured immediately after its execution were: critical temperature $T_c = 87.5 \text{ K}$, the temperature width of the superconducting transition $\Delta T_c = 1.4 \text{ K}$ and critical current $I_c \approx 550 \text{ mA}$ at 78 K [15]. The test sample was placed in a nitrogen flow-through cryostat designed for measurements in the temperature range from 77 to 300 K, fastening it to the "cold finger" with silver paste. During the measurements, the sample was in a vacuum of 10^{-2} hPa .

The research consisted in determining the voltage-current characteristics $U(I)$ of the HTS microbridge at

different temperatures and with different history of the preceding interactions. Measurements of $U(I)$ characteristics were carried out using the 4-wire method, supplying the microbridge from the current source. Such a supplying mode is more beneficial when testing the phenomenon of electro-resistance in comparison to the voltage source. This is due to the assumption (confirmed repeatedly in the literature, e.g. [6, 10]) that changes in resistivity may occur in different areas of the HTS structure by different physical mechanisms, and the total resistance of the microbridge can be treated as a serial connection of resistance of these areas. In such a model, with current stabilization, resistivity changes in one area do not cause changes in the electric field in neighbouring areas, which allows better identification of physical mechanisms depending on the intensity of this field. The measuring system uses the Keithley 2000 multimeter and the Keithley 6221 current source (which, in addition to direct current, can also generate periodic waveforms of the current). The measuring instruments were controlled by a PC via the GPIB interface.

On the basis of the obtained voltage-current characteristics, resistive-current characteristics $R(I)$ were determined. The maximum value of the current passed through the sample was 50mA, which is well below the level of the critical current I_c . In addition to measurements of $U(I)$ characteristics, measurements of the amplitude characteristics $R_o(U_m)$ of the resistive states of microbridge were also performed. The sample was subjected to quite long rectangular current pulses of varying amplitude I_m . As the amplitude U_m , the voltage was assumed on the sample at this current. The resistance R_o was determined after switching off the current - at the current $I_o = 10 \mu\text{A}$ assumed as the "zero" current. All measurements were carried out at room temperature ($T_a \approx 300\text{K}$) and the temperature of liquid nitrogen ($T_{LN} \approx 78\text{K}$).

Measurement results

The voltage-current characteristics were determined by changing the current in the range of $\pm 20 \text{ mA}$ in a stepped manner, keeping it at a given level for about 3 seconds, after which the voltage was measured. This cycle was repeated 3 times to ensure the repeatability of the characteristics. The positive direction was assumed conventionally due to the symmetry of the examined microbridge, and it was used consistently in all measurements. The measurements were carried out at room temperature T_a and after cooling to the temperature of liquid nitrogen T_{LN} . Between the measurements of the characteristics, the HTS microbridge was under a few minutes of DC current in various directions and values from 20 to 50 mA. On the basis of the obtained $U(I)$ dependences resistance-current characteristics $R(I)$ were determined.

Selected characteristics obtained in $T_a = 294\text{K}$ are shown in Fig.1a, while in $T_{LN} = 80\text{K}$ in Fig.1b. The order of measurements is in accordance with the numbering of the curves and the direction of the arrows marked on them. All characteristics are characterized by the presence of hysteresis (resistance hysteresis loop). If there is no current, HTS microbridge can be in two different resistance states: high R_H and low R_L . The $\pm 20 \text{ mA}$ current transfer switches the resistance between these states. These states are stable in the time scale of the measurements. We can therefore conclude that we are dealing with the phenomenon of electro-resistance memory and this is a non-volatile memory (memory states are kept in the absence of current). The resistance R_o of the microbridge in the non-current state ranges from 324 to 396 Ω in T_a , and

from 197 to 422 Ω in T_{LN} . Resistance changes $\Delta R_{HL} = R_H - R_L$ for a single hysteresis loop range from 8 to 74 Ω . The HTS microbridge resistance switching phenomenon is bipolar. At room temperature (Fig. 1a) under the influence of a positive current, the switching from high to low state ($R_H \rightarrow R_L$) occurs, and under the influence of negative current in the opposite direction ($R_L \rightarrow R_H$). The test results at the temperature of liquid nitrogen (Fig. 1b), however, indicate the opposite switching directions. When the positive current is active, the $R_L \rightarrow R_H$ is switched and at the negative current $R_H \rightarrow R_L$. The bipolarity of the resistance switching phenomenon also proves that it is not of a thermal nature.

In order to test the voltage necessary to switch the resistance, in parallel with the measurements of the voltage-current characteristics, measurements of the amplitude characteristics $R_o(U_m)$ of resistance states were also carried out. Through the HTS microbridge, the current of the course shown in Fig. 2 in the form of the I curve was passed. Rectangular current pulses had a variable amplitude value I_m in the range of $\pm 20 \text{ mA}$ and a constant component in the zero current level $I_o = 10 \mu\text{A}$. The duration of pulses and intervals between them was about 4s and resulted from the assumed measurement procedure and measurement time of the meters used. On the basis of the microbridge voltage waveforms measured during the current operation, its resistance curves (curve R in Fig. 2) were calculated, then the values R_o , R_m , I_m were read for a given current pulse, as shown in Fig.2. These values determined the coordinates of the point (U_m , R_o) of the amplitude characteristic of the resistance. Measurement of the entire characteristic took about 10 minutes.

Selected amplitude characteristics $R_o(U_m)$ obtained in studies conducted at T_a and T_{LN} temperatures are shown in Fig.3. Their course is similar to that obtained in the work of other authors, eg [6, 12]. Amplitude characteristics (Fig. 3), as well as resistance-current (Fig. 1) show that in the HTS microbridge there is a switching of resistance states under the influence of current interactions. Resistance values R_H , R_L and ΔR_{HL} are very similar to those shown in Fig.1. Also the directions of resistance switching in T_a and T_{LN} at the voltage with polarization corresponding to the current direction in Fig.1 are mostly the same. Only in the case of 3 (Fig. 3a), the switching directions were opposite than in other cases tested at room temperature. The obtained amplitude characteristics $R_o(U_m)$ clearly indicate the threshold character of the microbridge switching phenomenon. From their course, the values of switching voltage were determined at positive currents U_s^+ and negative U_s^- as shown in curve 2 (Fig.3a). The results obtained are summarized in Table 1.

Table 1. Resistance switching voltages at positive U_s^+ and negative U_s^- currents determined from the amplitude characteristics (Fig. 3).

Test no.	T	$U_s^+ [\text{V}]$	$U_s^- [\text{V}]$
2	T_a	1,0	3,8
3	T_a	4,1	4,2
6	T_{LN}	0,86	1,0
9	T_{LN}	0,92	0,90
11	T_{LN}	0,79	0,87
14	T_a	2,4	4,0

Switching voltages in all measurements carried out at the temperature of liquid nitrogen for both current directions are approximately equal to $0.8 \div 1.0 \text{ V}$. However, at room temperature they assume different values, from 1.0 to 4.2V. Furthermore, the values U_s for different current directions can be the same (measurement 3) or different (measurements 2, 14 in Figure 3a). Such differences of U_s^+ and U_s^- were also observed in the works [6, 16].

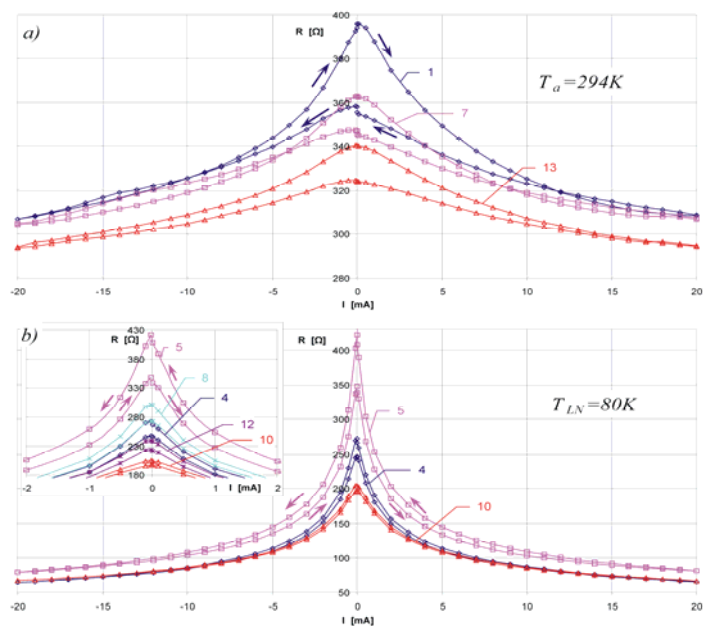


Fig.1. Resistance-current characteristics of HTS microbridge at room temperature (a) and temperature of liquid nitrogen (b). The order of measurements is consistent with the numbering of the curves and the direction of the arrows. On the insert - an enlarged fragment of the course around the zero current.

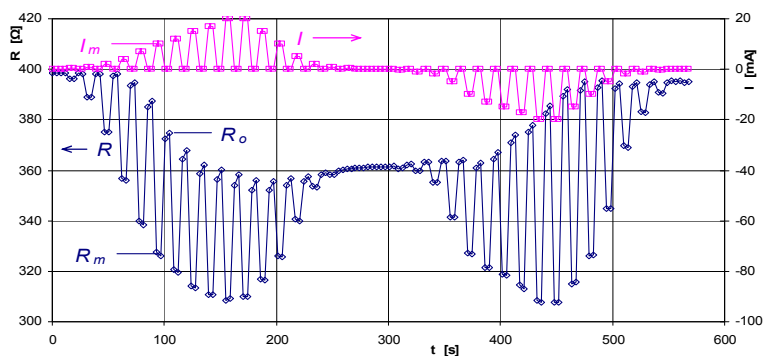


Fig.2. Waveforms of current I and resistance R of the HTS microbridge during the determination of amplitude characteristics.

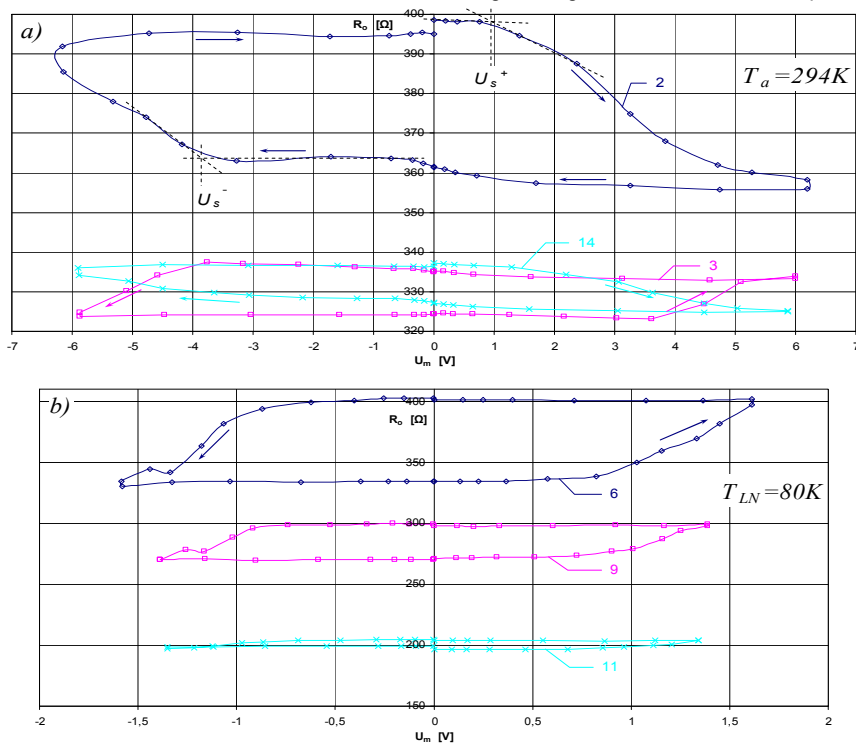


Fig. 3. The amplitude characteristics of the resistance states R_o of HTS microbridge at room temperature (a) and the temperature of liquid nitrogen (b). The order of measurements is consistent with the numbering of the curves and the direction of the arrows.

Analysis of results

The phenomenon of electro-resistance memory in oxide materials with a perovskite crystallographic structure is usually explained with the help of electrodiffusion of O^{2-} oxygen ions through oxygen vacancies [7, 10, 16-18]. Such materials are characterized by low activation energy of O^{2-} diffusion ($E_a = 0.7\text{eV}$) [7, 19] and high concentration of oxygen vacancies, which makes the probability of diffusion high. Oxygen diffusion inside and outside of the $\text{YBa}_2\text{Cu}_3\text{O}_{7-x}$ layer changes the oxygen deficit value x . The oxygen atoms in some of the elementary cell nodes serve as acceptor dopants. The increase in oxygen deficit leads to a decrease in the concentration of charge carriers (in high-temperature superconductors are holes) and, as a consequence, to an increase in resistivity (this relationship is very strong, because exponential [20]).

By reasoning analogously to [7, 10], it can be assumed that in the structure of our HTS microbridge, in the areas of $\text{YBa}_2\text{Cu}_3\text{O}_{7-x}$ adjacent to the Ag electrodes, there are oxygen depleted layers, i.e. high resistivity. Such layers arise in the normal technological process of producing high-temperature superconductors due to oxygen thermodiffusion to the environment [21, 22]. If we apply a positive potential to the electrode, high enough to provide O^{2-} ions with energy exceeding the diffusion activation energy (0.7eV), they will move through oxygen vacancies to the depleted layer, as a result of which the microbridge resistance will fall (R_L level). After switching off the voltage (current), the oxygen ions will stay in new positions, so the R_L state will be stable. With negative electrode polarization, the oxygen ions are pushed out of the near-electrode layer into the HTS material. This leads to the recovery of the depleted layer and the increase of resistance to the R_H level. The above-mentioned physical mechanism explains enough the phenomenon of HTS microbridge resistance switching between stable R_H and R_L levels, shown in Fig.1.

On the basis of this mechanism, it is also possible to explain different values of switching voltage U_s at different current directions observed in measurements 2 and 14 (table 1). To switch the resistance (in any direction), it is necessary to exceed the threshold value E_s of the electric field strength in the depleted layer. The $R_H \rightarrow R_L$ switching leads not only to the decrease in the resistivity of the depleted layer from the value of ρ_H to ρ_L , but also to the increase in the layer thickness ($d_H < d_L$). Switching in the opposite direction ($R_L \rightarrow R_H$) takes place by pushing O^{2-} ions through the electric field from the depleted layer into the material of the superconductor. However, in this case, to achieve the same field E_s , with a lower resistivity ρ_L , a larger switching current I_{sL} is needed than the previous I_{sH} ($E_s = \rho \cdot j$). In contrast, the switching voltage $U_{sL} = E_s \cdot d_L$ will be greater than the switching voltage U_{sH} due to the greater thickness d_L than d_H . It is in our measurements (2 and 14 in table 1) that $U_{sL} = U_{sH}$ is 3.8 and 4.0 V and is greater than $U_{sH} = U_{sL}$ equal to 1.0 and 2.4 V.

The above switching mechanism assumes a homogeneous diffusion of oxygen, namely along an axis perpendicular to the plane of the electrode. In the structures we examine, there may also be another mechanism taking place in the way of creating and destroying conductive filaments in the near-electrode layer [23, 24]. Such fibers are formed and disappear as a result of inhomogeneous electro-diffusion of oxygen ions in the region of the depleted layer. Then the switching voltage will be approximately the same for both directions ($U_{sL} \approx U_{sH}$), which is observed in measurements 3,6,9,11 (tab.1) of our research.

The clear difference in the resistance switching voltage U_s at room and liquid nitrogen temperature seen in Table 1 can be caused by the phase transition $N \rightarrow D$ (normal metal

state $N \rightarrow$ dielectric state D). This conversion occurs in $\text{YBa}_2\text{Cu}_3\text{O}_{7-x}$ at temperatures lower than 200K [7, 25-27]. It takes place through the loss of one atom of oxygen by the elementary cell, which makes it a $\text{YBa}_2\text{Cu}_3\text{O}_6$ cell with a tetragonal structure. This material is already a dielectric, an antiferromagnet with a strong order of oxygen atoms. The high activation energy E_a of the O^{2-} diffusion in the dielectric state means that the electro-diffusion in practice does not occur at the normally used bias voltages. If one cell loses an oxygen atom, then others will take it by becoming $\text{YBa}_2\text{Cu}_3\text{O}_7$ cells. This crystal is a degenerate p-type semiconductor with resistivity at the metal level. The phase transition $N \rightarrow D$ taking place in the depleted layer leads to a reduction in its thickness d , by switching off part of the layer from the O^{2-} ion electro-diffusion processes. On the other hand, as the temperature decreases, the activation energy E_a [7] also increases, which means that the E_s field necessary to switch the resistance is increased. The above changes d and E_s , taking place when lowering the temperature below 200K, can lead to both increase and decrease of the resistance switching voltage ($U_s = E_s \cdot d$). Our research has seen a decline, but in [6,7], the rise of U_s was also observed. A more detailed explanation of the mechanisms of changes in the resistance switching voltage requires additional testing.

Tomasek et al. [7] proposed a mathematical model of the resistance switching of the $\text{Ag}/\text{YBa}_2\text{Cu}_3\text{O}_{7-x}$ structure based on diffusion of O^{2-} ions in the field of oxygen vacancy potential. This field contains a system of narrow energetic barriers with the height equal to the activation energy E_a of oxygen diffusion, spaced from each other by λ equal to approximately the lattice constant in the plane ab . Application of this model allowed to determine the dependence of the resistance switching voltage U_s on the thickness d of the layer depleted in oxygen ions. Knowing the U_s from the amplitude characteristics of $R_o(U_m)$ (Fig. 3), the thickness of the depleted layer d can be determined from the relationship:

$$d = \frac{A_1 U_s}{E_a - A_2 T}$$

where: T - temperature, E_a - oxygen diffusion activation energy, A_1 and A_2 - constant values dependent on the microscopic parameters of O^{2-} ions diffusion in $\text{YBa}_2\text{Cu}_3\text{O}_{7-x}$. The values of A_1 and A_2 constants determined on the basis of the considerations contained in [7] are respectively: $1.28 \cdot 10^{-28} \text{ C} \cdot \text{m}$ and $2.10 \cdot 10^{-22} \text{ J/K}$. We adopt activation energy E_a equal to 0.7eV as the mean of the data presented in the literature for this material [7,20,21,28,29].

Thicknesses of depleted layers obtained in this way on the basis of data from table 1 are presented in table 2.

Table 2. Thicknesses of depleted layers d^+ and d^- calculated on the basis of switching voltages U_{s^+} and U_{s^-} from table 1.

Test no.	T	d^+ [nm]	d^- [nm]
2	T_a	2,6	9,6
3	T_a	10,4	10,6
6	T_{LN}	1,2	1,4
9	T_{LN}	1,2	1,2
11	T_{LN}	1,1	1,2
14	T_a	6,1	10,1

The thickness d^+ corresponds to the layer which is switched in our measurements with positive current and d^- with the negative current. At room temperature, d values were obtained in the range from 2.6 to 10.6 nm, while at the temperature of liquid nitrogen the value was approximately equal to 1.2 nm. Thus, the oxygen depleted layer has a thickness of 3 to 30 lattice constants of $\text{YBa}_2\text{Cu}_3\text{O}_{7-x}$ in the

plane ab , which are: $a \approx b \approx 4.4 \text{ \AA}$ [30]. Possible reasons for differences or equations d^+ and d^- , as well as differences in d values at T_a and T_{LN} temperatures are explained in the above analysis of the values of switching voltages U_s . From the Tomasek et al. [7] model shows that the temperature drop from T_a to T_{LN} causes the increase of the electric field intensity E_s from $4 \cdot 10^8$ to $7.4 \cdot 10^8$ V/m (i.e. about twice), which should cause a twice decrease in the thickness of the depleted layer. Meanwhile, our measurements show that the depleted layer decreased 10 times. This difference can be explained only by the participation of an additional mechanism, e.g. effects of the aforementioned phase transition $N \rightarrow D$. Thicknesses of the depleted layer presented in the literature for structures similar to ours range from 1 to 100nm [6-8,28]. The results obtained in our studies are therefore in line with the order of values with the above. Such a big dispersion of the value of d may result from different technologies of obtaining samples, as well as from various uncertainties of the obtained results, connected with fundamentally different measurement methods or even with the estimation calculations.

Summary

Conducted experimental investigations of the phenomenon of electro-resistance memory in $\text{Ag}/\text{YBa}_2\text{Cu}_3\text{O}_{7-x}/\text{Ag}$ thin-film structures allowed to determine the threshold values of the voltage of switching the resistance between two stable states. Differences in the levels of these voltages at different switching directions and at room and liquid nitrogen temperatures can be explained by a mechanism based on oxygen-ion electro-diffusion through oxygen vacancies. The application of the mathematical model of this mechanism allowed to determine the thickness of depleted layers in the studied structures, which play a fundamental role in the process of switching the resistance. The obtained thicknesses from 1.2 to 10.6 nm are consistent with the literature data for similar structures.

This paper was prepared at the Białystok University of Technology within a framework of the SWE/1/2013 project sponsored by the Ministry of Science and Higher Education, Poland.

Author: Jan Waśkiewicz, PhD, Eng. E-mail: j.waskiewicz@pb.edu.pl; Białystok University of Technology, Faculty of Electrical Engineering, ul. Wiejska 45d, 15-351 Białystok

REFERENCES

- [1] Freitas R.F., Wilcke W.W., Storage-class memory: The next storage system technology, *IBM J. Res. Dev.*, 52 (2008), 439.
- [2] Gastaldi R., Campardo G. (eds.), *In search of the next memory*, Springer IP AG, (2005).
- [3] Choi B.J., Jeong D.S., Kim S.K. et al., Resistive switching mechanism of TiO_2 thin films grown by atomic-layer deposition, *J. Applied Physics*, 98 (2005), 033715.
- [4] Hickmott T.W., *J. Applied Physics*, 33 (1962), 2669.
- [5] Gibbons J.F., Beadle W.E., *Solid-State Electron.*, 7 (1964), 785.
- [6] Acha C., Electric pulse-induced resistive switching in ceramic $\text{YBa}_2\text{Cu}_3\text{O}_{7-x}/\text{Au}$ interfaces, *Physica B*, 404 (2009), n.18, 2746-2748.
- [7] Tomasek M., Plecenik T., Truchly M. et al., Temperature dependence of the resistance switching effect studied on the metal/ $\text{YBa}_2\text{Cu}_3\text{O}_{6+x}$ planar junctions, *Journal of Vacuum Science and Technology B*, 29 (2011), n.1, 01AD04(1-5).

- [8] Plecenik T., Tomášek M., Belogolovskii M. et al., Effect of crystallographic anisotropy on the resistance switching phenomenon in perovskites, 111 (2012), n.5, 056106.
- [9] Waśkiewicz J., Gołębiowski J. Resistive memory physical mechanism in a thin-film $\text{Ag}/\text{YBa}_2\text{Cu}_3\text{O}_{7-x}/\text{Ag}$ structure, *Przeгляд Elektrotechniczny*, 91 (2015), n.11, 313-7.
- [10] Hanada A., Kinoshita K., Matsubara K. et al., Developmental mechanism for the resistance change effect in perovskite oxide-based resistive random access memory consisting of $\text{Bi}_2\text{Sr}_2\text{CaCu}_2\text{O}_{8+\delta}$ bulk single crystal, *Journal of Applied Physics*, 110 (2011), n.8, 084506(1-5).
- [11] Nian Y.B., Strozier J., Wu N.J. et al., Evidence for an oxygen diffusion model for the electric pulse induced resistance change effect in transition-metal oxides, *Physical Review Letters*, 98 (2007), 146403.
- [12] Acha C., Schulman A., Boudard M. et al., Transport mechanism through metal-cobaltite interfaces, *Applied Physics Letters*, 109 (2016), n.1, 011603.
- [13] Lee S.B., Kim A., Lee J.S. et al., *Appl. Phys. Lett.*, 97 (2010), 093505.
- [14] Acevedo W., Acha C., Sánchez M.J. et al., Origin of multistate resistive switching in Ti/manganite/ SiO_x/Si heterostructures, *Applied Physics Letters*, 110 (2017), n.5, 053501.
- [15] Gołębiowski J., Waśkiewicz J., Resistive memory effect in a thin-film structure based on $\text{YBa}_2\text{Cu}_3\text{O}_{7-x}$ superconductor, *Przeгляд Elektrotechniczny*, 89 (2013), n.8, 83-6.
- [16] Rozenberg M.J., Sanchez M.J., Weht R. et al., Mechanism for bipolar resistive switching in transition-metal oxides, *Physical Review B*, 81 (2010), n.11, 115101(1-5).
- [17] Tulina N.A., Borisenko I.Yu., Sirotkin V.V., Reproducible resistive switching effect for memory applications in heterocontacts based on strongly correlated electron systems, *Physics Letters A*, 372 (2008), n.44, 6681-6686.
- [18] Schulman A., Rozenberg M.J., Acha C., Anomalous time relaxation of the nonvolatile resistive state in bipolar resistive-switching oxide-based memories, *Physical Review B*, 86 (2012), n.10, 104426(1-5).
- [19] Taskin A.A., Lavrov A.N., Ando Y., Achieving fast oxygen diffusion in perovskites by cation ordering, *Applied Physics Letters*, 86 (2005), n.9, 91910-13.
- [20] Tu K.N., Yeh N.C., Park S.I. et al., *Physical Review B*, 39 (1989), 304.
- [21] Grajcar M., Plecenik A., Darula M., et al., Surface degradation of $\text{YBa}_2\text{Cu}_3\text{O}_{7-\delta}$ observed by means of contact resistance measurement, *Solid State Communications*, 81 (1992), n.2, 191-4.
- [22] Plecenik A., Grajcar P., Seidel P. et al., *Studies of high temperature superconductors*, 20 (1996), p.75.
- [23] Bruchhaus R., Waser R. Bipolar resistive switching in oxides for memory applications, *Thin Film Metal-Oxides: Fundamentals and Applications in Electronics and Energy*, (2010), pp.131-167.
- [24] Schulman A., Lanosa L.F., Acha C. Poole-Frenkel effect and variable-range hopping conduction in metal/ YBCO resistive switching, *Journal of Applied Physics*, 118 (2015), n.4, 044511 (1-6).
- [25] Lee P.A., Nagaosa N., Wen X.G., *Rev. Mod. Phys.*, 78 (2006), 17.
- [26] Plecenik A., Grajcar M., Seidel P. et al., *Physica C*, 301 (1998), 234.
- [27] Plecenik A., Grajcar P., Seidel P. et al., *Studies of high temperature superconductors*, 20 (1996), p.84.
- [28] Rothman S.J., Routbort J.L., Baker J.B., *Physical Review B*, 40 (1989), 8852.
- [29] Runde M., Routbort J.L., Rothman S.J. et al., *Physical Review B*, 45 (1992), 7375.
- [30] Plakida N.M., High temperature superconductivity: experiment and theory, Springer, Berlin, 1995, 237p.